Materials and Design 73 (2015) 1–9

Contents lists available at ScienceDirect

Materials and Design

journal homepage: www.elsevier.com/locate/matdes

Research on heat treatment of TiBw/Ti6Al4V composites tubes

Yang Yu [a,*], Wencong Zhang [a], Wenqian Dong [b], Xiuzhu Han [c], Chonglei Pei [a], Xueyan Jiao [a], Yangju Feng [a]

[a] School of Materials Science and Engineering, Harbin Institute of Technology at Weihai, No. 2, West Wenhua Road, Weihai 264209, Shandong Province, China
[b] Shanghai Spaceflight Precision Machinery Institute, No. 1, Guide Road, Songjiang District, Shanghai 201600, China
[c] Aerospace Research Institute of Materials & Processing Technology, Beijing 100076, China

ARTICLE INFO

Article history:
Received 4 January 2015
Accepted 21 February 2015
Available online 26 February 2015

Keywords:
Titanium matrix composites
TiB whisker
Hot-hydrostatic extrusion
Rotary swaging
Heat treatment

ABSTRACT

Heat treatment with different parameters were performed on the hot-hydrostatically extruded and swaged 3.5 vol.% TiBw/Ti6Al4V composites tubes. The results indicate that the primary α phase volume fraction decreases and transformed β phase correspondingly increases with increasing solution temperatures. The α + β phases will grow into coarse α phases when the aging temperature is higher than 600 °C. The hardness and ultimate tensile strength of the as-swaged TiBw/Ti6Al4V composite tubes increase with increasing quenching temperatures from 900 to 990 °C, while they decrease with increasing aging temperatures from 550 to 650 °C. A superior combination of ultimate tensile strength (1388 MPa) and elongation (6.1%) has been obtained by quenching at 960 °C and aging at 550 °C for 6 h. High temperature tensile tests at 400–600 °C show that the dominant failure modes at high temperatures also differ from those at room temperature.

1. Introduction

As a result of increasing demand in the aerospace, automotive and military applications for the excellent performance of structural materials, titanium matrix composites have been widely studied due to their high stiffness, toughness, elevated temperature resistance, high specific strength and low cost [1–5]. Among the various ways of producing reinforced titanium matrix composites, in situ synthesis techniques have attracted great attentions due to their superior properties. Various reinforcements including particles and whiskers can be used in titanium matrix composites, such as TiB, TiC, Al_2O_3, SiC, TiB_2 and rare earth oxides, for example, La_2O_3, etc. TiB is believed to be a very useful reinforcement due to its thermal stability and relative chemical stability in the Ti matrix according to previous researches [6–8]. In previous work [4,5], TiBw/Ti6Al4V composites with a novel network microstructure were successfully fabricated by tailoring the reinforcement distribution. Moreover, not only the strength but also the ductility of the novel composites is obviously improved compared with those with a homogeneous microstructure fabricated by the conventional powder metallurgy (PM) technology.

Undoubtedly, TiB whisker (TiBw) reinforced Ti6Al4V composites with network structure are preferable material for tubes applied in hydraulic pipelines for aerospace, nuclear power and automotive fields, especially high temperature fields.

Traditional hot-working technology, such as forging, extrusion and rolling, can be used to produce titanium matrix composites, such as sheet and bars. Over the past years, numerous studies have been carried out on the deformation of titanium and titanium alloys. It has been found that mechanical fibering (grains, second phases and inclusions aligned along the working direction) and texturing as a result of thermomechanical treatment have a great influence on the mechanical properties of materials [4,5,9–14].

However, there have been few reports on fabricating the thin-wall tube of TiBw reinforced titanium matrix composites [15]. As we know, it is difficult to perform plastic deformation on TMCs due to their high strength, hardness and modulus. Thus, an advanced plastic forming technology has been adopted to produce TiBw/Ti6Al4V composite tubes with thin wall. Many publications up to present have shown that hydrostatic extrusion is one of the most effective processes for deformation processing of difficult-to-deform materials [16–18]. Hydrostatic extrusion process is apparently advantageous over rolling and forging, because it can achieve a deformation amount as high as 60–90% in section area reduction by a single extrusion operation. At the same time, rotary swaging must be performed in order to fabricate slender thin-wall tubes of TiBw/Ti6Al4V composite after hot-hydrostatic extrusion.

Furthermore, subsequent heat treatment including solid solution and aging processes is also considered as one of the effective

* Corresponding author.
E-mail address: hityyang@hit.edu.cn (Y. Yu).

http://dx.doi.org/10.1016/j.matdes.2015.02.021
0261-3069/

strengthening methods which can further improve the strength of discontinuously reinforced titanium matrix composites by strengthening the titanium alloy matrix [8,19–22].

Therefore, it is important and necessary to investigate the effects of subsequent heat treatment on 3.5 vol.% TiBw/Ti6Al4V composites tubes fabricated by hot-hydrostatic extrusion and rotary swaging in order to further improve their mechanical properties.

2. Experimental

The spherical Ti64 powders and prismatic TiB_2 powders are chosen as raw materials in order to produce in situ 3.5 vol.% TiBw/Ti6Al4V (Ti64) composite tube. The average particle size of Ti64 powders is about 180 μm. Chemical composition (wt.%) and size distribution of Ti64 powders are listed in Tables 1 and 2, respectively. Then both powders were milled in planetary ball mill (QM-2SP12) at speed of 200 rpm for a period of 8 h, using argon as protective atmosphere. The weight ratio of balls to powders is 5:1. The morphology of Ti64, TiB_2 and milled powders are shown in Fig. 1. Subsequently, the hot-pressing sintering technology was carried out in vacuum (10^{-2} Pa) at 1200 °C for 1 h under the load of 20 MPa. The reinforcements of the titanium matrix composites were in situ synthesized according to the reaction:

$$Ti + TiB_2 = 2TiB \quad (1)$$

Table 1
Chemical composition (wt.%) of Ti64 powders.

Al	V	Cl	Na	Fe	Si	O	C	N	H	Ti
6.42	4.12	–	–	0.18	0.024	0.12	0.013	0.011	0.004	Bal.

Table 2
Size distribution of Ti64 powders.

Particle size (μm)	>178	178–150	150–104	104–89	89–74	74–44	<44
Proportion (%)	1.84	30.13	50.66	5.34	7.03	4.6	0.34

Then the sintered billets were subjected to a hot-hydrostatic extrusion with an extrusion ratio of about 10.56 (reduction of area about 90.53%) at 1000–1200 °C and the tubes were fabricated with external and internal diameters of 16 and 10 mm, respectively. Glass powders of softening temperature 1100 °C were used as lubricant during hot-hydrostatic process. Then, the as-extruded tubes were swaged at 950 °C with 15% reduction of area during each swaging pass. After swaging, the tubes with 7 mm in external diameter and 2 mm in thickness were produced finally. Both the extrusion processes were performed on a 4-column hydraulic press with a pressing velocity of about 15 mm/s. 3.5 vol.% TiBw/Ti64 composite tubes after grinding were shown in Fig. 2.

In order to further investigate the effects of the subsequent heat treatment on the microstructure and mechanical properties of 3.5 vol.% TiBw/Ti64 composites tubes, heat treatment were performed on the as-swaged composite tubes. As referred in previous work [23], the α phase of Ti64 alloy begins to transform to β phase at 600 °C and thoroughly transforms to β phase at 985 °C. When the quenching temperature is higher than 800 °C, partial β phase can transform to martensite phase. Therefore, the water quenching (WQ) temperature was carried out at 900–990 °C and aging at 500–650 °C.

Thus, solution and aging treatments were performed following the hot rotary swaging process. In the present study, 900, 930, 960 and 990 °C were selected as solution temperatures followed by water quenching (WQ), and the aging temperatures were 500,550, 600 and 650 °C for 6 h followed by air cooling (AC).

Samples for metallographic observations were cut directly from the composites. The samples were then prepared using the conventional techniques of grinding, polishing and subsequent etching using the Kroll's solution (5 vol.% HF + 10 vol.% HNO_3 + 85 vol.% deionized H_2O) for 10 s. Metallographic observations of the specimens were performed on an OLYMPUS GX71 optical microscope (OM). X-ray diffractions (XRD) using Cu Kα radiation (λ = 0.1546 nm) were performed on an XD-2700 equipment along the longitudinal direction of the as-extruded and as-swaged specimens to identify the phases. Scanning electron microscopy (SEM) observation was carried out with a Hitachi S-570 scanning electron microscope equipped with energy dispersive spectroscopy (EDS) system. Vickers hardness tests were carried out on an HVS-1000 micro Vickers hardness tester. The test load was 1000 g and time

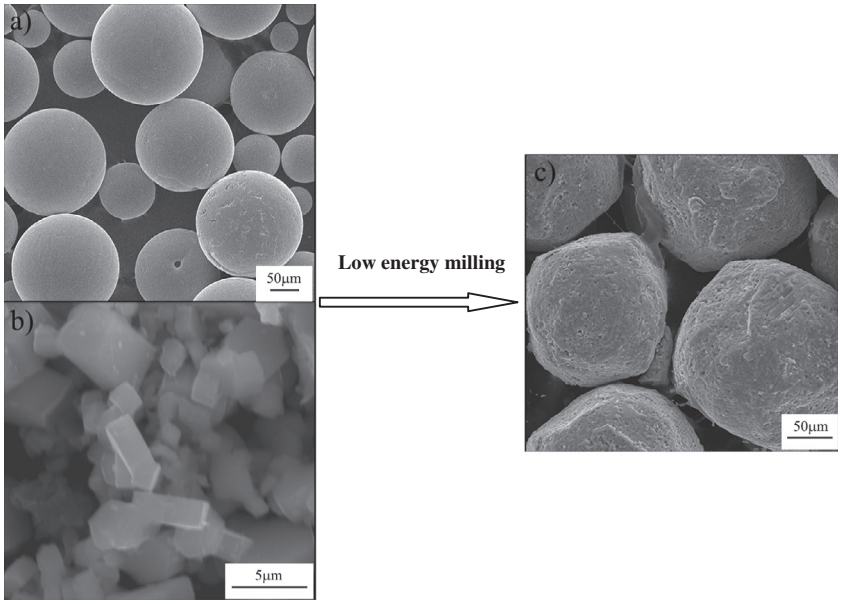

Fig. 1. The morphology of experimental powders. (a) Ti64 powders, (b) TiB_2 powders and (c) milled powders.

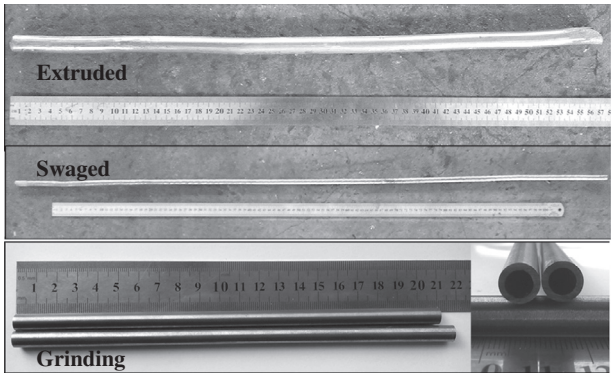

Fig. 2. TiBw/Ti64 composite tubes with different processing states.

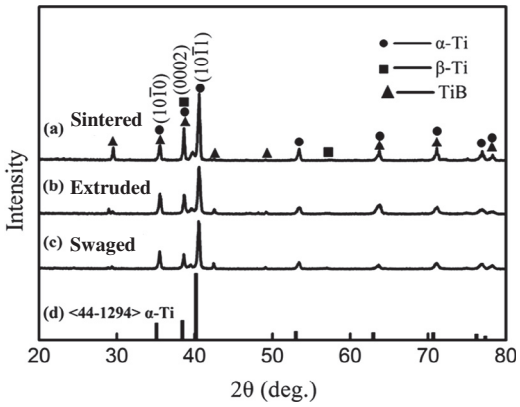

Fig. 4. XRD patterns of the 3.5 vol.% TiBw/Ti64 composites with different processing states.

of packing was 10 s. Hardness was obtained by measuring the diagonal distance of indentation. Each specimen after being polished on the cross section was tested 9 times at different positions and the average value was obtained (on the cross section of as-swaged TiBw/Ti6Al4V composites tubes, the region of indentation covered both titanium matrix and the TiB whiskers). Tensile tests at room temperature and high temperature were carried out on an Instron-5569 and Instron-1186 universal test machines, respectively, driven at constant crosshead speed of 0.5 mm/min (the identical strain rate is 5.5×10^{-4}/s). Room temperature tensile samples were cut from the as-sintered composite by wire-electrode cutting equipment and dimensions were reported in our previous work [15]. The shapes and dimensions of tube tensile specimens are shown in Fig. 3. At least four tests were performed on each condition and average values were reported.

3. Results and discussions

3.1. Microstructure

Fig. 4 displays the XRD patterns of the sintered, extruded and swaged 3.5 vol.% TiBw/Ti64 composites (tubes) compared with the standard XRD pattern of a titanium powder (PDF44-1294). As shown in the figure, TiB phase has been synthesized in the sintered composites and maintained during the process. Meanwhile, the intensity of some specific peaks of TiB changed apparently after extrusion and swaging, suggesting a preferred orientation generated for TiB. As for the matrix, the intensity of the peaks after the extrusion and swaging was similar to that of the standard a titanium card, but comparatively a slight increase for the intensity of the $(10\bar{1}0)$ peak was observed after the extrusion and then decrease after the swaging process. XRD patterns of the 3.5 vol.% TiBw/Ti64 composites are similar to our previous work because of using the same sintering and hot-hydrostatic extrusion techniques. Compared with our previous work [15], rotary swaging at 950 °C was used to produce composites tubes in this study instead of near-β extrusion at 950 °C. In addition, it is clear that whisker-like (about 1.5 μm in width) phase enriched with B (as determined by EDS) formed a typical network structure around Ti64 matrix particles after vacuum hot-pressing sintering, as mentioned in previous work [15].

Fig. 5 shows the optical micrographs of TiBw/Ti64 composites with different extrusion temperatures. As can be seen clearly, the transverse sections of the deformed composites also retain quasi-equiaxed morphology. TiB whiskers became fine and disperse after hot-hydrostatic extrusion due to severe plastic deformation. Additionally, the Ti64 matrix of the as-sintered TiBw/Ti64 composites exhibits the quasi-equiaxed α + β microstructure as reported in the previous work [4,5,15] and the phase transformation diagram of Ti64 alloy [23]. Because the extrusion temperature is higher than the β extrusion deformation above the β transformation temperature of 985 °C. According to the previous research [24], dynamic recrystallization and grain refinement are also formed during the hot deformation. After extrusion, the grain size of Ti64 matrix and original β phase were considerably refined and the average width of α phase decreased. These deformed microstructures are beneficial to the tensile properties of the matrix and thereby those of the composites. And this will be proved by the tensile properties as mentioned below. But the α phase and β phase become coarse with the increasing extrusion temperature due to dynamic recrystallization. As compared with Fig. 5(a) and (b), there was no significant difference. But hot-hydrostatic extrusion performed at 1000 °C need larger deformation load. Whereas the hot-hydrostatic extrusion process was performed at 1200 °C, coarse β phase and inferior surface quality of TiBw/Ti64 composites tubes would be acquired. Based on this, the β extrusion temperature of 1100 °C may be optimized in this experiment.

In consideration of phase transformation, high plasticity and low flow stress at elevated temperature, near-β swaging temperature of 950 °C was selected. Fig. 6(a) reveals that TiB whiskers were oriented along the longitudinal direction after the rotary swaging deformation. The laminar α phase and β phase were observed along the cross section as shown in Fig. 6(b). And this result is very similar to Wang's [13].

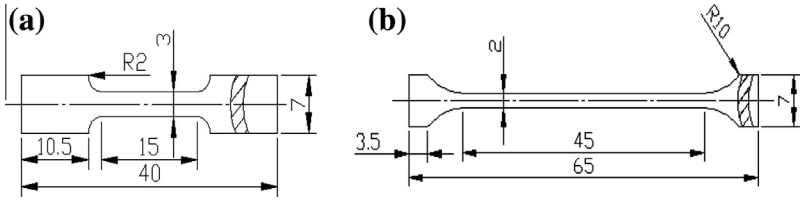

Fig. 3. Dimensioned schematic of the tubes tensile specimen. (a) Room temperature specimen and (b) high temperature specimen, mm.

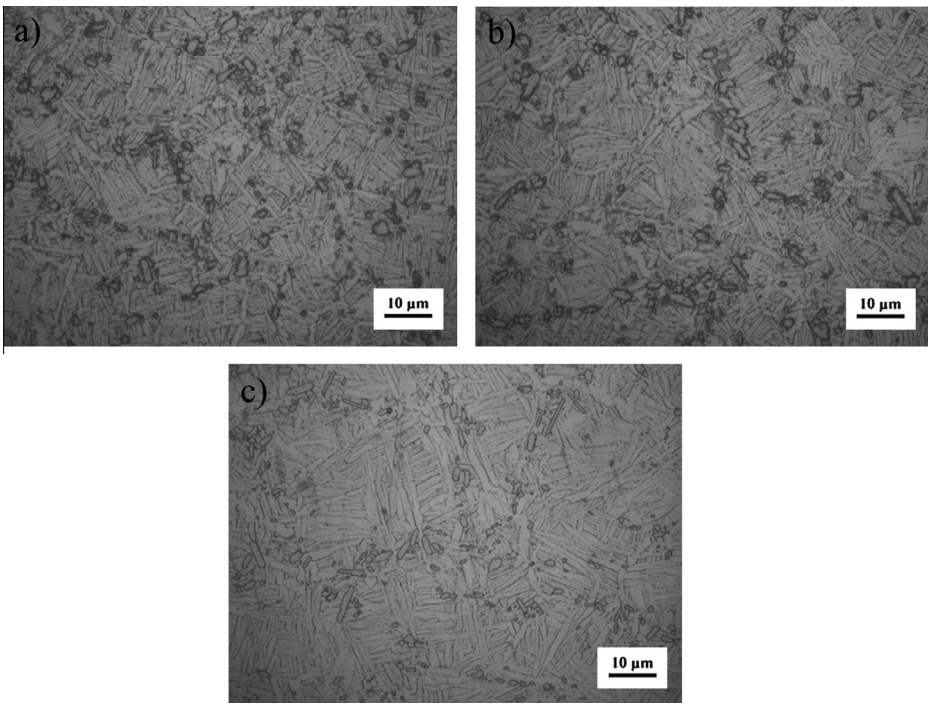

Fig. 5. Optical micrographs of TiBw/Ti64 composites tubes along the transverse section with different extrusion temperatures. (a) 1000 °C, (b) 1100 °C and (c) 1200 °C.

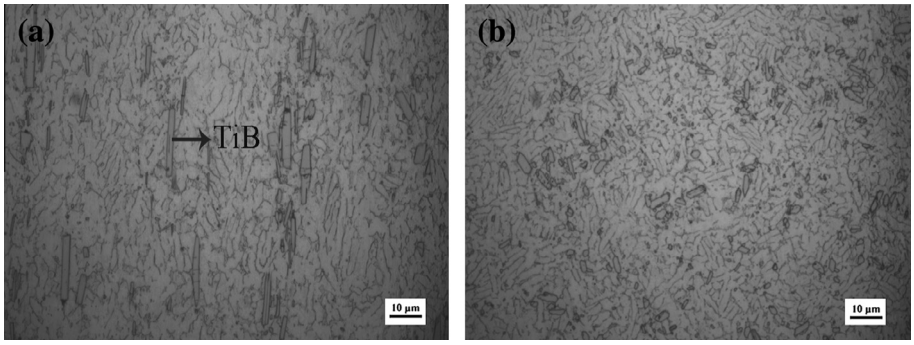

Fig. 6. OM micrographs of as-swaged TiBw/Ti64 composites tubes. (a) Along the longitudinal section and (b) along the transverse section.

Fig. 7 shows OM images along the transverse section of the as-swaged TiBw/Ti64 composites tubes followed by water quenching at 900–990 °C. During the solution treatment process, the primary α phase continuously transforms into the β phase at phase transformation temperature. Some of the high temperature β phase converted into needle-shaped martensite α′ phase during the cooling process, and the others remained as the residual β phase. The transformed β phase constituting of α′ phase and the residual β phase is formed during the solution treatment and WQ processes [25]. With increasing solution temperature, the volume fractions of the primary laminate α phase decreases and that of the transformed β phase increases as shown in Fig. 7. Because the α phase of Ti64 matrix alloy thoroughly transforms to β phase at 985 °C [23], the laminate α phase have completely transformed into β phase at 990 °C, as shown in Fig. 8(d).

Fig. 8 shows the SEM micrographs of the as-swaged TiBw/Ti64 composite tubes quenched at temperatures of 900, 930, 960 and 990 °C and aged at 500 °C for 6 h. Comparing with Fig. 6, the volume fraction of the transformed β phase in the heat-treated composites is much higher than that of the β phase in the as-swaged composites tubes. Fig. 8 also indicates that the volume fraction of the transformed β phase increases with increasing solution temperatures. The α + β phases formed from martensite α′ phase during the aging process are well-distributed in the transformed β phase in which the brighter fine phase is β phase. The volume fraction of the fine α + β phases increases with increasing solution temperature. This indicates that with increasing quenching temperatures the volume fraction of martensite α′ phase increases, while the fraction of the residual β phase in the transformed β phase decreases due to lower aging temperature, which is beneficial to the hardness and the strength of the composites tubes. It seems that fine α + β phases will be acquired with increasing aging temperature at certain solution temperature.

Fig. 9 shows the SEM micrographs of the as-swaged TiBw/Ti64 composites tubes quenched at 960 °C and aged at different temperatures for 6 h. In Fig. 9(a), there is a small amount of needle-shaped martensite α′ phase. Whereas little martensite α′ phase and more dispersive α + β phases can be seen in Fig. 9(b). It also can be seen that the size of the fine α + β phases increases with increasing aging temperatures and the fine α + β phases will grow into coarse phases when the aging temperature is higher than 600 °C as shown in Fig. 9(c) and (d). It is certain that the coarsening

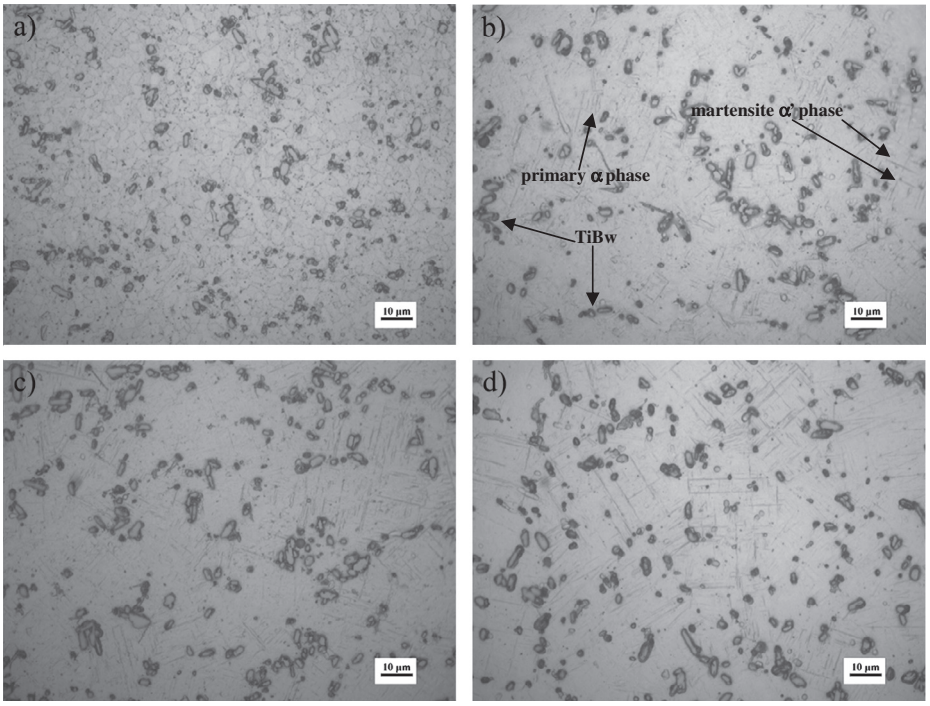

Fig. 7. OM micrographs of the as-swaged TiBw/Ti64 composites tubes quenched with different temperatures. (a) 900 °C, (b) 930 °C, (c) 960 °C and (d) 990 °C.

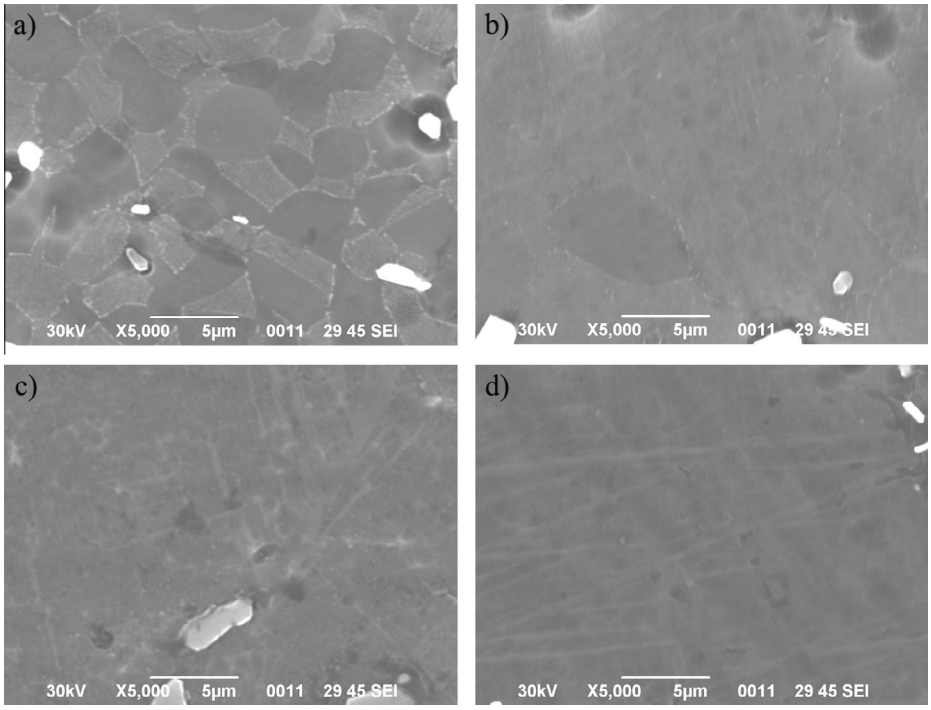

Fig. 8. SEM micrographs of the as-swaged TiBw/Ti64 composites tubes quenched with different temperatures followed by aging at 500 °C for 6 h. (a) 900 °C, (b) 930 °C, (c) 960 °C and (d) 990 °C.

α + β phases are harmful to hardness and strength of the Ti6Al4V matrix. Additionally, the size of the primary α phases lightly grows after the aging process, as seen by comparing Figs. 8 with 9(a), and then increases with increasing aging temperatures as shown in Fig. 9. This phenomenon indicates that the martensite α′ phase along the edge of the primary α phase is prior formed into the stable α + β phase. The laminate α phase with a larger size is observed by integrating the disintegrated a phase with the primary α phase, which may be beneficial to the ductility of the composites tubes [13].

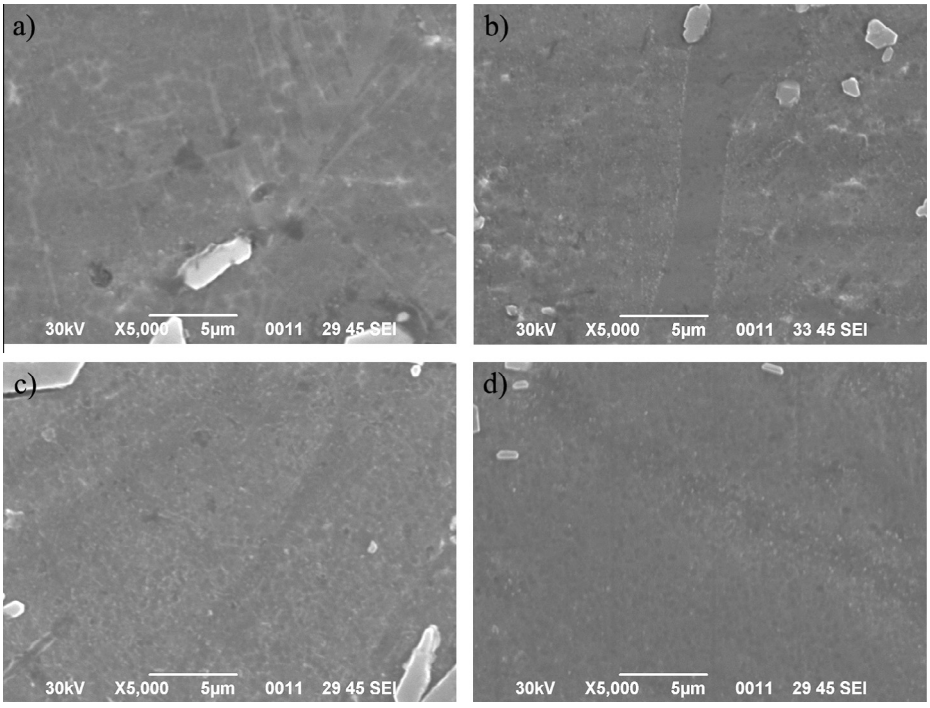

Fig. 9. SEM micrographs of the as-swaged TiBw/Ti64 composites tubes quenched at 960 °C and aged at different temperatures for 6 h. (a) 500 °C, (b) 550 °C, (c) 600 °C and (d) 650 °C.

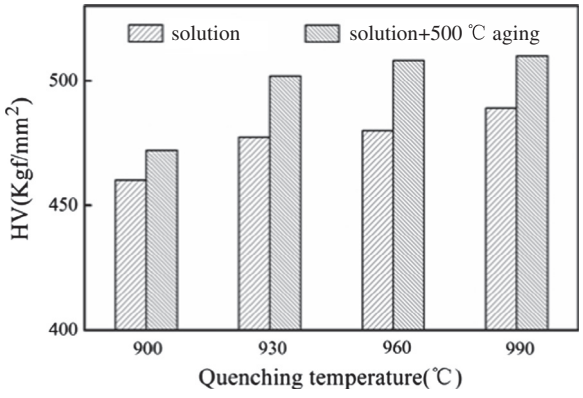

Fig. 10. Vickers hardness of TiBw/Ti64 composites tubes quenched at different temperatures and aged at 500 °C for 6 h.

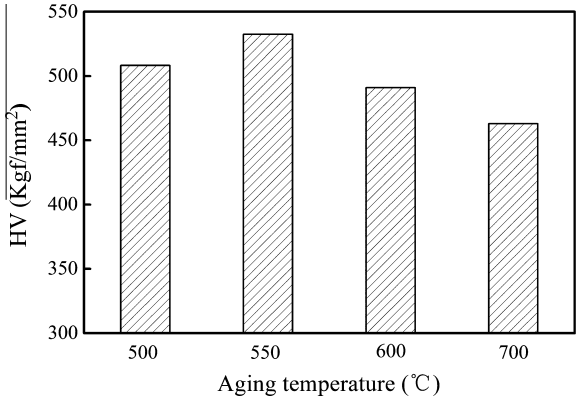

Fig. 11. Vickers hardness of as-swaged TiBw/Ti64 composites tubes quenched at 960 °C and aged at different aging temperatures.

3.2. Mechanical properties

Fig. 10 shows the Vickers hardness of TiBw/Ti64 composites tubes quenched at different temperatures and aged at 500 °C for 6 h. It can be seen that the hardness increases with increasing quenching temperatures. And the Vickers hardness of as-aged TiBw/Ti64 composite tubes is higher than that of the as-solution. The Vickers hardness even reached 489 kg f/mm^2 for the sample quenched at 990 °C, while it was 460 kg f/mm^2 for the sample quenched at 900 °C. Compared with value 449 kg f/mm^2 of as-swaged tubes, the Vickers hardness of quenched tubes at 900–990 °C increased obviously. Whereas the Vickers hardness of TiBw/Ti64 composites tubes quenched at a range of temperatures from 900 to 990 °C and aged at 500 °C for 6 h can reach 472, 501, 508, and 510 kg f/mm^2, respectively. The reason for the increasing hardness can be interpreted as follows: firstly, the volume fraction of the transformed β phase increases with increasing quenching temperatures in the range of the two α + β phases area. Secondly, the fraction of the martensite α′ phase in the transformed β phase increases with increasing quenching temperatures because of the decreasing amount of β phase elements in the transformed β phase. Additionally, the increased fraction of the martensite α′ phase can also further increase the fraction of fine α + β phases, thereby increasing the aging strengthening effect.

Fig. 11 shows the Vickers hardness of as-swaged TiBw/Ti64 composites tubes quenched at 960 °C and aged at 500 °C, 550 °C, 600 °C and 650 °C. It can be clearly seen that the hardness of the

Table 3
Room-temperature tensile properties of TiBw/Ti64 composites.

Processing states of TiBw/Ti64 composites	UTS (MPa)	Elongation (%)
As-sintered	1051.0	6.5
As-extruded	1272.0	9.1
As-swaged	1221.0	11.8
As-heat treated	1388.0	6.1

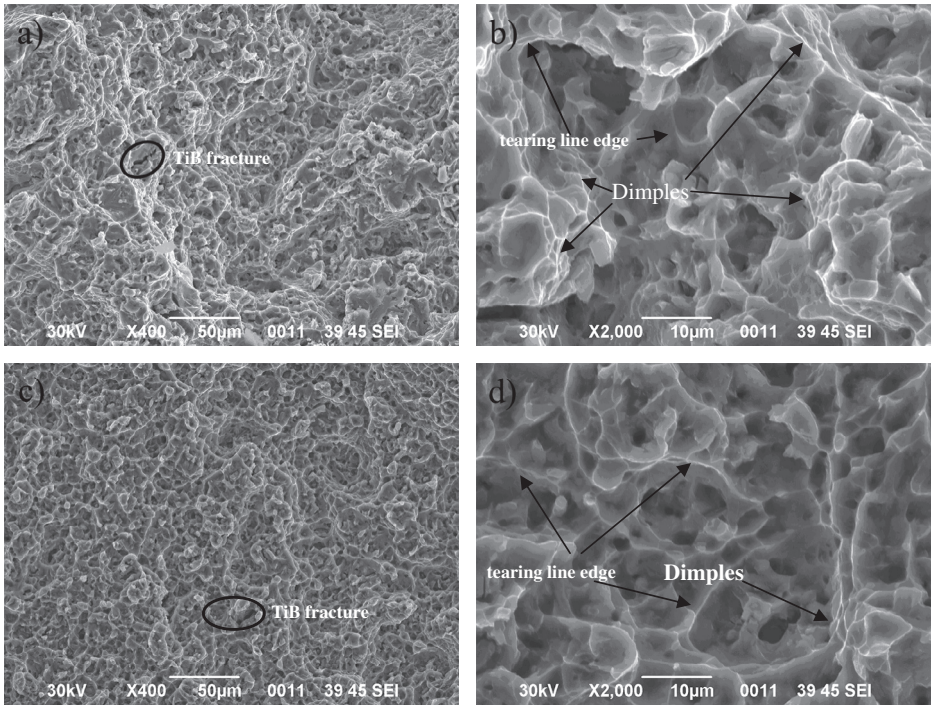

Fig. 12. Room-temperature tensile fracture micrographs of the TiBw/Ti64 composites tubes with different processing states. (a) The as-extruded at low magnification, (b) the as-extruded at high magnification, (c) the as-swaged at low magnification and (d) the as-swaged at high magnification.

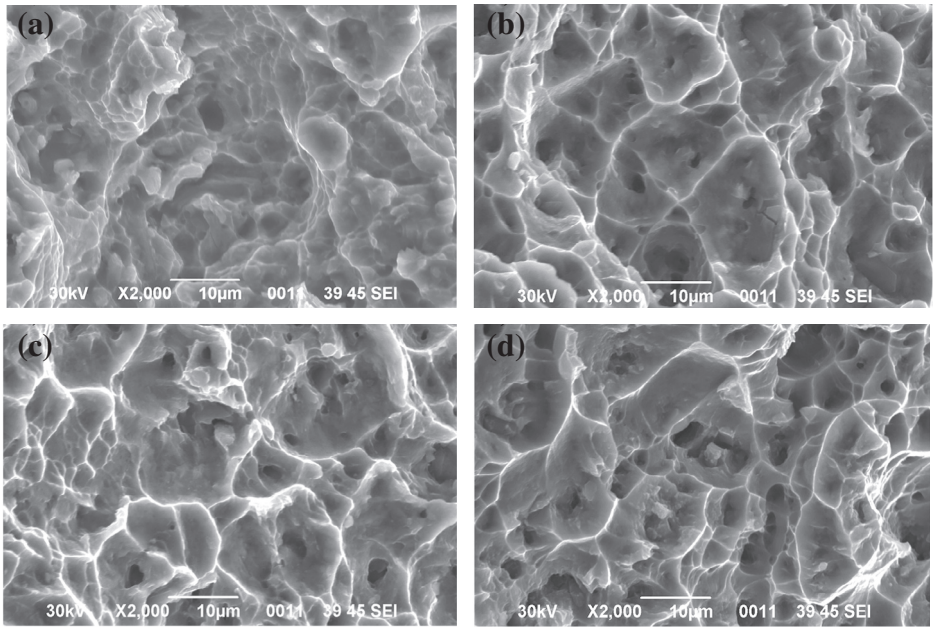

Fig. 13. Room and high temperature tensile fractographs of the as-swaged 3.5 vol.% TiBw/Ti64 composite tubes heat treated by 960 °C/30 min/WQ + 550 °C/6 h/AC. (a) Room temperature, (b) 400 °C, (c) 500 °C and (d) 600 °C.

samples reaches the maximum value aged at 550 °C. Then the hardness of the samples decreases from 532 to 463 kg f/mm^2 when the aging temperature is higher than 550 °C. The reason is that the fine $\alpha + \beta$ phases grow into coarse phases with increasing aging temperature which can be proved by Fig. 9.

Thus, heat treatment parameters in this study were selected as followed: water quenching (WQ) was carried out at 960 °C for 30 min and aging at 550 °C air cooled (AC) for 6 h.

Room temperature tensile properties of TiBw/Ti64 composites are listed in Table 3. The tensile strength and the tensile elongation of the as-swaged tubes compared with the as-sintered composite are increased by 16.2% and 81.5%. The three main reasons for the significant improvement of the deformed composites ductility are as following: the local volume fraction of reinforcement on the network boundary decreases after extrusion and swaging deformation; the deformed column matrix is distributed along

Table 4
High-temperature properties of TiBw/Ti64 composites tubes after water quenching at 960 °C and aging at 560 °C for 6 h.

Temperature (°C)	UTS (MPa)	Elongation (%)
400	991.0	11.2
500	895.0	14.5
600	635.0	19.3

the extruded direction; the grain size of matrix is refined during severe plasticity deformation process, especially the rotary swaging. The increment of strength can be mainly attributed to the matrix strain hardening including the formation of martensite, dislocation, twinning, texture, dynamic recrystallization and grain refinement [4]. In the research of Gungor [26], β extrusion was used to produce seamless Ti6Al4V tubes with ultimate tensile strength of 960 MPa, yield strength of 857 MPa and elongation of about 13%.

It is certain that the alignment distribution of TiB whisker reinforcement is beneficial to the improvement of the strength. Thus, the strength can be further increased from 1221 MPa of the as-swaged composite tubes to 1388 MPa after heat treatment due to the formation of the transformed β phase, as shown in Table 3. But the tensile fracture elongation is remarkably decreased from 11.8% to 6.1%. This phenomenon can be attributed to the formation of the transformed β phase including the martensite phase.

The high temperature tensile properties of the as-swaged composite tubes treated by 960 °C/30 min/WQ + 550 °C/6 h/AC are shown in Table 3. The strength is remarkably decreased from 991 MPa at 400 °C to 895 MPa at 500 °C and 635 MPa at 600 °C, respectively. On the contrary, the tensile elongation is significantly increased from 11.2% at 400 °C to 14.5% at 500 °C and 19.3% at 600 °C, respectively. This is mainly due to the matrix softening [23].

3.3. Fracture characteristics

The cracked TiB whiskers and some small facets are observed in the fracture surfaces of the as-sintered 3.5 vol.% TiBw/Ti64 composite [15], indicating a brittle cleavage fracture mode of the as-sintered composite. The results are also consistent with the inferior ductility of the as-sintered composites.

Fig. 12 shows the room temperature tensile fractographs of the as-extruded and the as-swaged composite tubes. As shown in Fig. 12, it is in contrast to Fig. 11 where not only fractured TiB whiskers but also many dimples and matrix tearing line edges are found in the fracture surface, implying the fracture type changes from brittle cleavage fracture to the coexistence of plastic fracture and brittle fracture. It is further confirmed that the as-extruded and the as-swaged composites can exploit a superior ductility mainly due to matrix grain refinement.

Fig. 13 shows the high temperature tensile fractographs of the as-swaged composite tubes after heat treatment. According to Fig. 13, the heat-treated tubes tested at 400–600 °C show typical ductile fracture surfaces with a lot of dimples. The results are also consistent with the superior ductility and inferior strength of the composite tubes, shown in Table 4. The superior ductility of the specimen can be attributed to the good plasticity of the matrix at high temperatures.

4. Conclusions

Heat treatments with different parameters were performed on the as-swaged 3.5 vol.% TiBw/Ti6Al4V composites tubes in order to further increase their mechanical properties and reveal the microstructure and performance evolution. The present work has led to the following findings:

(1) Compared with the as-sintered 3.5 vol.% TiBw/Ti6Al4V composites, not only the strength but also the ductility of the composites tubes can be significantly increased by the hot-hydrostatic extrusion and rotary swaging.
(2) The primary α phase volume fraction decreases and transformed β phase correspondingly increases with increasing solution temperatures. Both the size and volume fraction of α + β phases formed from the quenched martensite α′ phase increase with elevated aging temperature, and they will grow into coarse α phases when the aging temperature is higher than 600 °C.
(3) The high temperature strength is remarkably decreased and the tensile elongation is significantly increased with the increasing of temperature. The heat-treated 3.5 vol.% TiBw/Ti64 composite tubes tested at 400–600 °C show typical ductile fracture surfaces with a lot of dimples.

Acknowledgements

This study was supported by the National High-Tech Research and Development Program of China (“863 Program”, No. 2013AA031202), the aerospace science and technology innovation fund of China Aerospace Science and Technology Corporation (Grant No. pb(s)-2014-4), the Natural Scientific Research Innovation Foundation in Harbin Institute of Technology (Project No. HIT.NSRIF.2011108).

References

[1] M. Zadra, L. Girardini, High-performance, low-cost titanium metal matrix composites, Mater. Sci. Eng., A 608 (2014) 155–163.
[2] W.J. Lu, D. Zhang, X.N. Zhang, R.J. Wu, T. Sakata, H. Mori, Creep rupture life of in situ synthesized (TiB + TiC)/Ti matrix composites, Scripta Mater. 44 (2001) 2449–2455.
[3] D.B. Miracle, Metal matrix composites-from science to technological significance, Compos. Sci. Technol. 65 (15–16) (2005) 2526–2540.
[4] L.J. Huang, L. Geng, A.B. Li, F.Y. Yang, H.X. Peng, In situ TiBw/Ti–6Al–4V composites with novel reinforcement architecture fabricated by reaction hot pressing, Scripta Mater. 60 (11) (2009) 996–999.
[5] L.J. Huang, L. Geng, H.X. Peng, J. Zhang, Room temperature tensile fracture characteristics of in situ TiBw/Ti6Al4V composites with a quasi-continuous network architecture, Scripta Mater. 64 (9) (2011) 844–847.
[6] K. Morsi, V.V. Patel, Processing and properties of titanium–titanium boride (TiBw) matrix composites – a review, J. Mater. Sci. 42 (6) (2007) 2037–2047.
[7] C.J. Boehlert, S. Tamirisakandala, W.A. Curtin, D.B. Miracle, Assessment of in situ TiB whisker tensile strength and optimization of TiB-reinforced titanium alloy design, Scripta Mater. 61 (2009) 245–248.
[8] S. Gorsse, D.B. Miracle, Mechanical properties of Ti–6Al–4V/TiB composites with randomly oriented and aligned TiB reinforcements, Acta Mater. 51 (9) (2003) 2427–2442.
[9] X.L. Guo, L.Q. Wang, M.M. Wang, J.N. Qin, D. Zhang, W.J. Lu, Effects of degree of deformation on the microstructure, mechanical properties and texture of hybrid-reinforced titanium matrix composites, Acta Mater. 60 (2012) 2656–2667.
[10] S.L. Semiatin, V. Seetharaman, I. Weiss, Flow behavior and globularization kinetics during hot working of Ti–6Al–4V with a colony alpha microstructure, Mater. Sci. Eng., A 263 (1999) 257–271.
[11] W. Schillinger, A. Bartelsa, R. Gerling, F.-P. Schimansky, H. Clemens, Texture evolution of the γ- and the α/α_2-phase during hot rolling of γ-TiAl based alloys, Intermetallics 14 (2006) 336–347.
[12] L.J. Huang, L. Geng, B. Wang, H.Y. Xu, B. Kaveendran, Effects of extrusion and heat treatment on the microstructure and tensile properties of in situ TiBw/Ti6Al4V composite with a network architecture, Composites: Part A 43 (2012) 486–491.
[13] B. Wang, L.J. Huang, L. Geng, Effects of heat treatments on the microstructure and mechanical properties of as-extruded TiBw/Ti6Al4V composites, Mater. Sci. Eng., A 558 (2012) 663–667.
[14] H.T. Hu, L.J. Huang, L. Geng, C. Liu, B. Wang, Effects of extrusion on microstructure and tensile properties of 3D network structured TiBw/Ti60 composites fabricated by reaction hot pressing, J. Alloys Comp. 582 (2014) 569–575.

[15] W.C. Zhang, X.Y. Jiao, Y. Yu, J.L. Yang, Y.J. Feng, Microstructure and properties of 3.5 vol.% TiBw/Ti6Al4V composite tubes fabricated by hot-hydrostatic extrusion, J. Mater. Sci. Technol. 30 (2014) 710–714.
[16] Z.H. Zhang, F.C. Wang, Research on the deformation strengthening mechanism of a tungsten heavy alloy by hydrostatic extrusion, Int. J. Refract. Met. Hard Mater. 19 (2001) 177–182.
[17] N. Inoue, M. Nishara, Hydrostatic Extrusion-Theory and Application, Elsevier, Amsterdam, 1985.
[18] Y. Yu, L.X. Hu, E.D. Wang, Microstructure and mechanical properties of a hot-hydrostatically extruded 93W–4.9Ni–2.1Fe alloy, Mater. Sci. Eng., A 435–436 (2006) 620–624.
[19] J.X. Li, L.Q. Wang, J.N. Qin, Y.F. Chen, W.J. Lu, D. Zhang, The effect of heat treatment on thermal stability of Ti matrix composite, J. Alloys Comp. 509 (2011) 52–56.
[20] X.J. Tian, S.Q. Zhang, H.M. Wang, The influences of anneal temperature and cooling rate on microstructure and tensile properties of laser deposited Ti–Al–1.5Mn titanium alloy, J. Alloys Comp. 608 (2014) 95–101.
[21] Z.G. Zhang, J.N. Qin, Z.W. Zhang, Y.F. Chen, W.J. Lu, D. Zhang, Effect of β heat treatment temperature on microstructure and mechanical properties of in situ titanium matrix composites, Mater. Des. 31 (2010) 4269–4273.
[22] P. Majumdar, S.B. Singh, S. Dhara, M. Chakraborty, Influence of in situ TiB reinforcements and role of heat treatment on mechanical properties and biocompatibility of β Ti-alloys, J. Mech. Behav. Biomed. Mater. 10 (2012) 1–12.
[23] G. Welsch, R. Boyer, E.W. Collings, Materials Properties Handbook: Titanium Alloys, ASM International, 1994.
[24] L.J. Huang, L. Geng, A.B. Li, G.S. Wang, X.P. Cui, Effects of hot compression and heat treatment on the microstructure and tensile property of Ti–65Al–3.5Mo–1.5Zr–0.3Si alloy, Mater. Sci. Eng., A 489 (2008) 330–336.
[25] L.J. Huang, H.Y. Xu, B. Wang, Y.Z. Zhang, L. Geng, Effects of heat treatment parameters on the microstructure and mechanical properties of in situ TiBw/Ti6Al4V composite with a network architecture, Mater. Des. 36 (2012) 694–698.
[26] M.N. Gungor, I. Ucok, L.S. Kramer, H. Dong, N.R. Martin, W.T. Tack, Microstructure and mechanical properties of highly deformed Ti–6Al–4V, Mater. Sci. Eng., A 410–411 (2005) 369–374.